NCAT Report 11-06

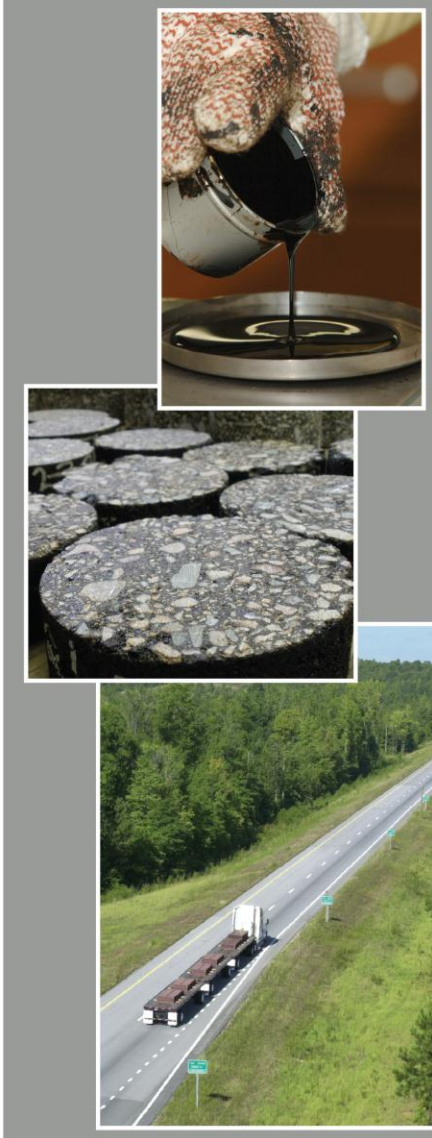

EVALUATION OF WARM MIX ASPHALT IN WALLA WALLA, WASHINGTON

By
Courtney Jones
Randy West
Grant Julian
Adam Taylor
Graham Hurley
Andrea Kvasnak

October 2011

National Center for Asphalt Technology
NCAT
at AUBURN UNIVERSITY

277 Technology Parkway ■ Auburn, AL 36830

EVALUATION OF WMA IN WALLA WALLA, WASHINGTON

DRAFT FINAL REPORT

By

Courtney Jones
Randy West
Grant Julian
Adam Taylor
Andrea Kvasnak
National Center for Asphalt Technology
(AMRL Certification Number 251)
and
Graham Hurley
Advanced Materials Services, LLC

Sponsored by
Maxam Equipment, Inc.
Andy Welch
816-241-7380
awelch@maxamequipment.com

NCAT Report 11-06

October 2011

DISCLAIMER

The contents of this report reflect the views of the authors who are responsible for the facts and accuracy of the data presented herein. The contents do not necessarily reflect the official views or policies of Maxam Equipment, the National Center for Asphalt Technology, or Auburn University. This report does not constitute a standard, specification, or regulation.

ABSTRACT

A warm-mix asphalt (WMA) field demonstration was conducted in Walla Walla, Washington in April 2010 to compare conventional hot-mix asphalt (HMA) with WMA produced using the AquaBlack^{TM} asphalt foaming system developed by Maxam Equipment, Inc. The National Center for Asphalt Technology (NCAT) documented the production and construction of the demonstration projects and evaluated both mixes using a range of state-of-the-art laboratory tests. Results of the comparison are detailed in this report.

TABLE OF CONTENTS

1. INTRODUCTION

Interest in the use of warm-mix asphalt (WMA) has grown faster than any other new asphalt technology in the past several decades. WMA technologies allow the complete coating of aggregates, placement, and compaction at lower production temperatures. Although the reduction in temperature varies by technology, WMA is generally produced at temperatures ranging from 35°F lower than hot-mix asphalt (HMA) to the approximate boiling point of water (212°F). Simply put, these technologies are workability and compaction aids.

The benefits of WMA include reduced emissions, reduced fuel usage, reduced binder oxidation, and paving benefits such as the potential for equivalent densities at lower temperatures compared to HMA, cool-weather paving, and longer haul distances. To assure these benefits are fully realized and that WMA provides expected pavement performance, proper construction practices must be utilized. Although most aspects of designing and constructing WMA are similar to HMA, lower production temperatures and binder modifications associated with WMA could result in differences in pavement performance relative to HMA (*1*).

This report documents the construction and materials evaluation of a WMA demonstration in Walla Walla, Washington. The WMA technology used on this project was an asphalt foaming system using water injection developed by Maxam Equipment. This WMA technology is referred to by the trade name AquaBlack^{TM}. The WMA and HMA were produced and placed on a new section of US-12. The estimated two-way AADT for this section of roadway was approximately 11,000 vehicles per day with 17% trucks. The production of the WMA and companion HMA control took place on April 19 and 20, 2010.

2. MIX DESIGN

The asphalt mixture used for this trial consisted of a coarse-graded 12.5-mm nominal maximum aggregate size (NMAS) Superpave mix design, with a compactive effort of 100 gyrations. The mix design used for the HMA was also used for the WMA without any changes. The aggregate used for the design was a basalt and natural sand blend including 20% reclaimed asphalt pavement (RAP). The materials percentages used for mix design submittal and production are shown in Table 1. The Washington State Department of Transportation (WSDOT) allows the substitution of up to 20% RAP without the use of blending charts. The asphalt mixture used a PG 64-28 asphalt binder supplied by Idaho Asphalt Company. A liquid anti-stripping agent, Unichem 8162, manufactured by BJ Services Company, was added to the asphalt binder at a rate of 0.25% by weight of liquid binder. The design aggregate gradation, optimum asphalt content, design volumetrics, specifications, and allowable tolerances are shown in Table 2. It should be noted that the design was done without RAP, as is common in the state of Washington.

Table 1 Aggregate Percentages Used in Mix Design

Aggregate Type	%, Mix Design	%, Production

Coarse Chips	21	12
Fine Chips	76	62
Natural Sand	3	6
RAP	0	20

Table 2 Design Gradation, Asphalt Content, and Volumetrics for Mix Design

Sieve Size, mm (in.)	Percent Passing, %	Specifications	Tolerances
19.0 (3/4")	100	100	99-100
12.5 (1/2")	94	90-100	90-100
9.5 (3/8")	81	90 Max	75-87
4.75 (#4)	52		47-57
2.36 (#8)	34	28-58	30-38
1.18 (#16)	23		
0.6 (#30)	16		
0.3 (#50)	12		
0.15 (#100)	8		
0.075 (#200)	5.6	2.0-7.0	3.6-7.0
AC, %	5.2	0-10	4.7-5.7
Air Voids, %	3.7	2.5-5.5	2.5-5.5
VMA, %	14.7	14 Min	12.5 Min
VFA, %	75	65-75	65-75
D/A Ratio	1.2	0.6-1.6	0.6-1.6

The WMA was produced using the AquaBlack™ WMA system developed by Maxam Equipment, Inc. This system, shown in FIGURE 1, uses a foaming gun (enlarged for detail on the right side of the figure) to create foaming. For this field trial, water was added at a rate of 2.5% by weight of the virgin asphalt binder.

FIGURE 1 Maxam AquaBlack™ WMA System

3. PRODUCTION

For the WMA, 2,286 tons were produced, while 1,974 tons of HMA were produced the following day. Production temperature for the WMA was approximately 275°F (135°C), and for the HMA control, production temperature was approximately 325°F (163°C). The asphalt plant used to produce the asphalt mixtures was a portable, parallel-flow Cedar Rapids drum mix plant that incorporated a Hauck SJO-580 Starjet burner. The plant used natural gas as fuel and incorporated a single 60-ton silo. FIGURE 2 shows the asphalt plant used for this field trial.

FIGURE 2 Granite Northwest — Walla Walla, WA Portable Asphalt Plant

During the production of the WMA, the average production rate for the entire day was approximately 307 tph (tons per hour), with a range of 226 to 342 tph. Production of the WMA using PG 64-28 as the binder stopped for approximately an hour, so that WMA using PG 70-28 could be produced. This was done to allow paving through an intersection on the roadway. No plant settings were altered, so data recording continued through the production of WMA with the PG 70-28. The initial loader used to feed the aggregate cold-feed bins broke down toward the end of production, so a second, smaller, loader was used; this reduced the production rate from 335 tph down to 230 tph.

For the HMA, the average production rate was approximately 316 tph, with a range of 265 to 334 tph. About an hour into production, the mix transfer device on the roadway broke down, causing a 1.5-hour delay. When production resumed, HMA using PG 70-28 was produced to allow paving through an intersection, as was done with the WMA. During production of the HMA, dust control became an issue; therefore, the pulse time in the baghouse was increased by one second. It was believed that the water in the baghouse waste auger system could not thoroughly mix with the baghouse dust due to the high temperature of the baghouse dust, allowing dust to flow freely from the end of the waste auger. However, this was not an issue during the production of the WMA because of the reduced temperature of the baghouse dust. At about 280°F, the baghouse dust could fully mix with the water in the waste auger system, where it could be easily controlled. This is shown in FIGURE 3.

FIGURE 3 Waste Auger System for Baghouse, Showing Full Mixing of Water and Dust

Samples of each mixture were obtained during production to compare moisture contents, percent coating, and volumetric properties between the HMA and WMA. Complete production test results are presented in Appendix A.

3.1 Mix Moisture Content

AASHTO T 329, *Moisture Content of Hot Mix Asphalt (HMA) by Oven Method*, was used to evaluate the moisture content of loose plant-produced mix (two samples per mix per day). The temperature stipulated in AASHTO T 329 was not used due to limited oven space in the NCAT mobile laboratory, which prevented one oven being used solely for moisture-content testing. The oven temperature was set to the target compaction temperature plus 20°F. This was the temperature needed to get the gyratory samples to reach compaction temperature quickly. Each sample was approximately 5000 g. The samples were heated to a constant weight (less than 0.05% change), as defined by AASHTO T 329.

The average moisture contents were 0.07% and 0.23% for the HMA and WMA, respectively. These results are well below the allowable maximum moisture content in WSDOT specifications. A higher moisture content of about 0.1% was expected for the WMA due to the addition of water for foaming (2.5% by weight of virgin asphalt binder which is about 0.1% by weight of total mix). It is possible the higher moisture content of the WMA may also have been partially due to the lower mix production temperature for WMA, which could have left some residual moisture in the aggregate or RAP going

through the plant. However, is more likely that the difference in moisture content is also influenced by testing variability.

3.2 Coating

AASHTO T 195, *Determining Degree of Particle Coating of Asphalt Mixtures*, commonly known as a Ross count, was used to evaluate asphalt coating of the loose plant-produced mix (one sample per mix per day). Mix obtained from truck samples was sieved over a 3/8 in. (9.5 mm) sieve. Visual inspections of the particles retained on the 3/8 in. (9.5 mm) sieve were conducted, which consisted of classifying a particle as partially or completely coated. The percent of completely coated particles was then calculated. The percent of coated particles was 99.3% for the HMA and 100.0% for the WMA. Thus, the WMA and HMA exhibited similar coating characteristics.

3.3 Volumetrics

Specimens were compacted using 100 gyrations of the Superpave gyratory compactor (SGC) at compaction temperatures of 300°F for the HMA samples and 250°F for the WMA samples. Water absorption levels were low (<2%), therefore bulk specific gravity (G_{mb}) was determined in accordance with AASHTO T 166. Solvent extractions were conducted in accordance with AASHTO T 164, and the recovered binder was graded according to AASHTO R 29. Average test results are summarized in Table 3, and complete test results are presented in Appendix A. The intermediate binder grade for each mix was reported between the high and low binder grades, as shown in

Table 3.

The gradation results for both the HMA and WMA were within the job mix formula (JMF) tolerances. The asphalt content of the WMA (5.11%) was close to the JMF (5.2%), and while the asphalt content of the HMA (5.66%) was higher than the WMA but was still within the acceptable range of 5.2 ± 0.5%. The percentage of absorbed asphalt was also higher for the HMA than the WMA. However, the air voids of both mixes were equivalent and met the specifications. The recovered binder true grades were very similar.

Table 3 Gradation, Asphalt Content, and Volumetrics for Plant-Produced Mix

	HMA	**WMA**	**JMF**
Sieve Size	**Average % Passing**		**% Passing**
25.0 mm (1")	100.0	100.0	100
19.0 mm (3/4")	100.0	100.0	100
12.5 mm (1/2")	94.0	95.4	94
9.5 mm (3/8")	80.1	81.0	81
4.75 mm (#4)	51.9	49.5	52
2.36 mm (#8)	33.4	31.3	34
1.18 mm (#16)	23.2	21.9	23
0.60 mm (#30)	17.6	16.8	16
0.30 mm (#50)	14.3	13.8	12
0.15 mm (#100)	9.5	9.7	8
0.075 mm (#200)	6.0	6.6	5.6
Asphalt Content (%)	5.66	5.11	5.2
G_{mm}	2.606	2.597	--

G_{mb}	2.517	2.509	--
V_a (%)	3.4	3.4	3.7
P_{ba} (%)	1.15	0.63	--
Recovered Binder True Grade	77.9 + 21.6 - 26.0	75.3 + 20.6 - 27.9	--

4. WEATHER

Weather data was collected hourly at the paving location using a handheld weather station. The ambient temperature during the WMA paving ranged between 54.2°F and 87°F (12.3°C and 30.5°C), while the ambient temperature during the HMA paving ranged between 75.6°F and 80.2°F (24.2°C and 26.8°C). The wind during the WMA paving was between 0 and 2.1 mph, and for the HMA paving, between 0 and 9.6 mph. The humidity during the WMA paving was between 33.7 to 68.9%. The humidity during the HMA paving was between 26.5 and 38.2%. There was no rain during the paving of either mix.

5. CONSTRUCTION

A new section of US-12 was built approximately parallel to the existing roadway (*2*). The produced WMA and HMA were placed as the surface course on the new construction. The WMA was placed in the passing lane and the HMA in the traveling lane. Figure 4 illustrates the placement on the sections. The WMA section monitored for this project began before the HMA section. The green flag on the map indicates the location of asphalt plant. The target thickness was 1.5 inches. A tack coat was applied at a rate of 0.11 gal/yd^2 prior to laying the surface lift using a CSS-1 supplied by Idaho Oil.

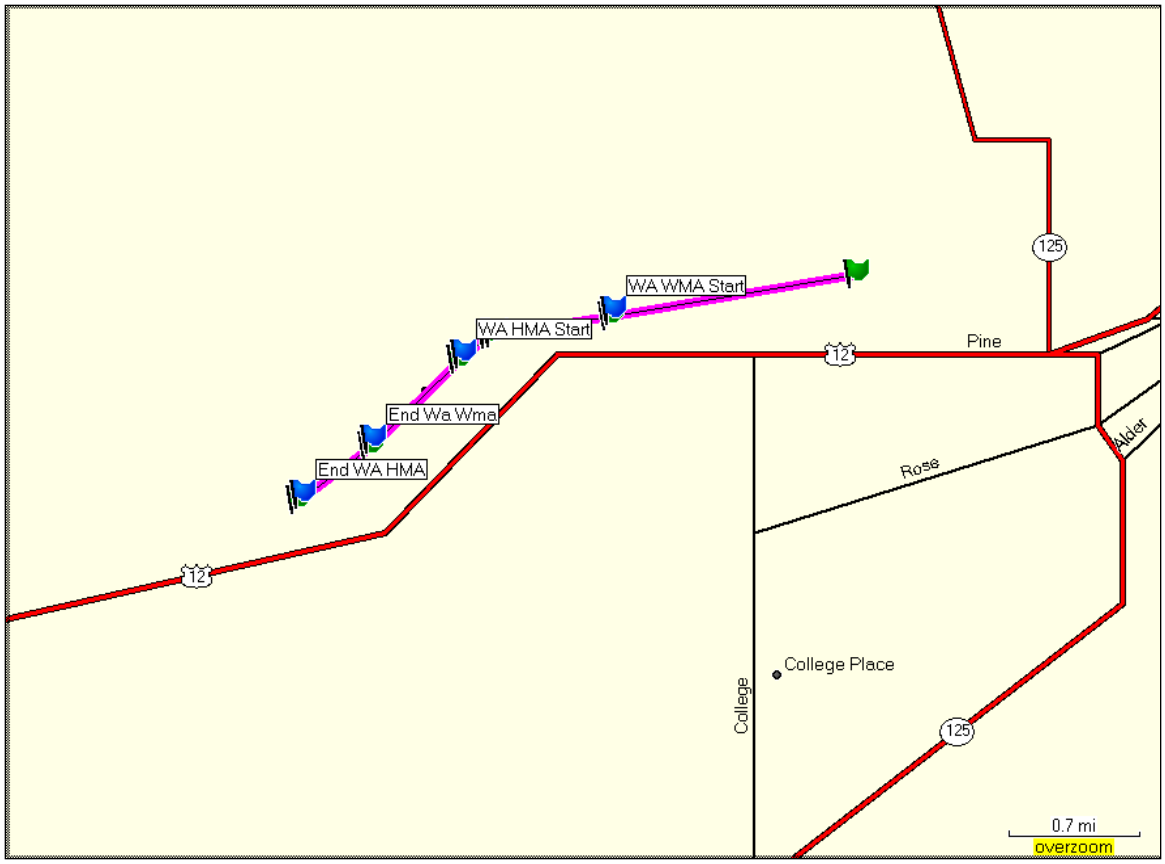

Figure 4 Location of WMA and HMA sections

The asphalt mixtures were delivered using tarped belly-dump trucks. Maxi-Kreme, manufactured by Global-Chem Source, was used as a release agent to prevent asphalt sticking to the truck beds. A cycle of five trucks delivered the material to the roadway. The haul distance from the plant to the roadway was less than five miles, so there was little production stoppage due to lack of trucks during the day.

The belly-dump trucks discharged the mix into windrows. The delivery temperature of the WMA ranged between 244 and 259°F while the HMA ranged between 272 and 295°F. A RoadTec SB-2500D material transfer vehicle (MTV) was used to collect the windrowed mix (see Figure 5 and Figure 6). It should be noted that on the HMA construction day, the shuttle buggy broke down and construction was delayed until the shuttle buggy could be repaired. The delay at the paving site was approximately 1.5 hours.

Figure 5 Material Transfer Vehicle

Figure 6 Material Transfer Device and Windrow

The MTV discharged the mix into a Blaw-Knox PF 6110 paver (see Figure 7). The screed heater was on during WMA and HMA construction, set to 250°F and 270°F during WMA and HMA construction, respectively. The temperature of the WMA behind

the screed ranged from 246 to 255°F. The HMA mat temperature behind the screed was between 251 and 287°F.

The mix was compacted using three rollers. The WMA breakdown roller was an Ingersoll Rand DD 130HF set at an amplitude setting of 3, while the HMA breakdown roller was an Ingersoll Rand DD 138 set at a amplitude setting of 3. A different breakdown roller was used for the HMA since the roller used on the WMA section was mistakenly transported to another site. The difference in rollers was not due to expected changes in compaction. The intermediate roller was a Caterpillar PS 360C with a tire pressure between 90 and 100 psi. The finishing roller was an Ingersoll Rand DD 110HP, which was operated in the static mode. The rolling pattern was the same for both mixes.

Figure 7 Blaw-Knox Paver

The temperature behind the paver was monitored using temperature probes, which collected temperature data every 30 seconds. Data from the probes were processed to determine the rate at which the mat cooled. Regression was used to fit a model to the mat temperature and time data collected. Figure 8 illustrates the regression cooling models developed for WMA and HMA. Based on the data collected, the WMA cooled at a slower rate than the HMA.

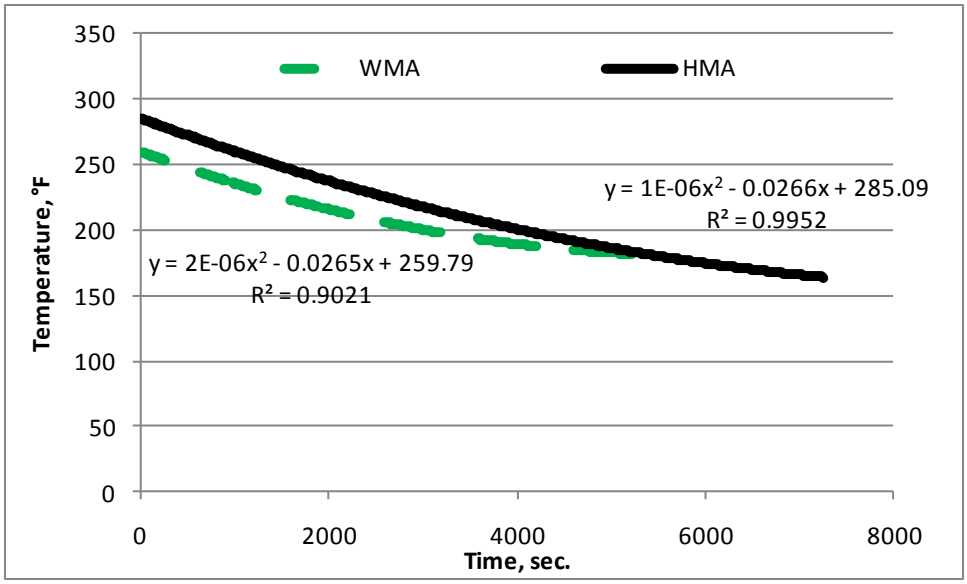

Figure 8 Mix Cooling Trend

6. CORE TESTING

Field cores were obtained from each section (WMA and HMA) following compaction. Core densities were determined in accordance with AASHTO T 166. Five cores were tested for tensile strength, and additional cores were combined for solvent extraction (AASHTO T 164) and gradation analysis. Average test results are shown in TABLE 4, and complete test results are presented in Appendix B.

Gradation results for both mixes were very similar. As was the case with the results from the plant mix during production, the asphalt content of the HMA cores (5.69%) was higher than that of the WMA cores (4.87%). The asphalt content of the HMA cores was very close to the plant mix asphalt content (5.66%), while the asphalt content of the WMA cores was slightly less than that of the WMA plant mix (5.11%). The difference between the core and field mix asphalt contents for the WMA can probably be attributed to testing variability. Average core densities were similar for both mixes, at 94.6% of theoretical maximum density (TMD) for the HMA and 94.4% of TMD for the WMA. Tensile strengths and recovered binder true grades were similar for both the HMA and WMA.

TABLE 4 Core Test Results

	HMA	WMA
Sieve Size	**% Passing**	
25.0 mm (1")	100.0	100.0
19.0 mm (3/4")	100.0	100.0
12.5 mm (1/2")	96.6	94.1
9.5 mm (3/8")	84.5	82.5
4.75 mm (#4)	56.3	54.5
2.36 mm (#8)	37.4	37.2
1.18 mm (#16)	27.2	27.5
0.60 mm (#30)	21.2	21.8
0.30 mm (#50)	17.5	18.1
0.15 mm (#100)	11.5	11.8
0.075 mm (#200)	7.3	7.3
Asphalt Content (%)	5.69	4.87
G_{mm}	2.598	2.606
G_{mb}	2.459	2.459
V_a (%)	5.4	5.6
P_{ba} (%)	1.04	0.62
Tensile Strength (psi)	160.9	165.4
Recovered Binder True Grade	72.9 + 22.2 - 26.1	75.7 + 19.2 - 25.9

Note: Gradation and asphalt content results are based on one sample per mix.

7. MIX PROPERTY TESTING

Selected mix tests were conducted to assess moisture susceptibility, strength, permanent deformation, stiffness, fatigue, and compactability. Table 5 summarizes the tests used to evaluate the mixes. The results of the WMA were compared to the HMA to determine if the lab properties were similar to the HMA.

Table 5 Tests Conducted on Plant-Produced Mix

Test	Mix Property Evaluated	Replicates
Dynamic Modulus (AASHTO TP 79)	Stiffness	3 Specimens per Mix
Moisture Susceptibility (AASHTO T 283)	Moisture Susceptibility	3 Unconditioned, 3 Conditioned per Mix
Hamburg Wheel-Tracking Test (AASHTO T 324)	Moisture Susceptibility and Rutting Resistance	3 Twin Sets per Mix
Beam Fatigue (AASHTO 321)	Fatigue Resistance	6 per mix (2 strain levels)
Thermal Cracking (AASHTO T 322)	Thermal-Cracking Resistance	3 Specimens per Mix
Flow Number Confined (AASHTO TP 79)	Permanent-Deformation Resistance	3 Specimens per Mix
Flow Number Unconfined (NCHRP 09-43 Method)	Permanent-Deformation Resistance	3 Specimens per Mix

7.1 Dynamic Modulus

The stiffness of the mixes was evaluated using the dynamic modulus test outlined by AASHTO TP 79-09, *Standard Method of Test for Determining the Dynamic Modulus and Flow Number for Hot-Mix Asphalt (HMA) Using the Asphalt Mixture Performance Tester (AMPT).* The testing was performed in an IPC Global ® AMPT device (Figure 9). The specimens for this testing were prepared from re-heated plant-produced mix according to the tolerances set by AASHTO PP60-09, *Preparation of Cylindrical Performance Test Specimens Using the Superpave Gyratory Compactor (SGC)*. Three specimens per mix were compacted using a gyratory compactor to a height of 175 mm. These specimens were then cored with a 100-mm core drill and cut to yield 150-mm tall specimens. The target air-void content of the final prepared samples was 7 ± 0.5%.

Figure 9 IPC Global®Asphalt Mixture Performance Tester

The testing frequencies and temperatures were those recommended by AASHTO PP61-09, *Developing Dynamic Modulus Master Curves for Hot Mix Asphalt (HMA) Using the Asphalt Mixture Performance Tester (AMPT)*. A high test temperature of 40^{o}C was selected based on the virgin binder grade used for the HMA and WMA. The confining pressure employed was 20 psi (138 kPa). The data from the dynamic modulus test was used to create a master curve. The mastercurve uses the principle of time-temperature superposition to correct collected data at multiple temperatures and frequencies to a reference temperature so that stiffness data can be viewed without temperature as a variable. A visual example of this principle is shown as Figure 10. The data analysis methodology is that listed by AASHTO PP61-09. There is no standard pass/fail criterion for these data; therefore, the master curves of the dynamic modulus developed from the testing were used to compare WMA stiffness to that of HMA.

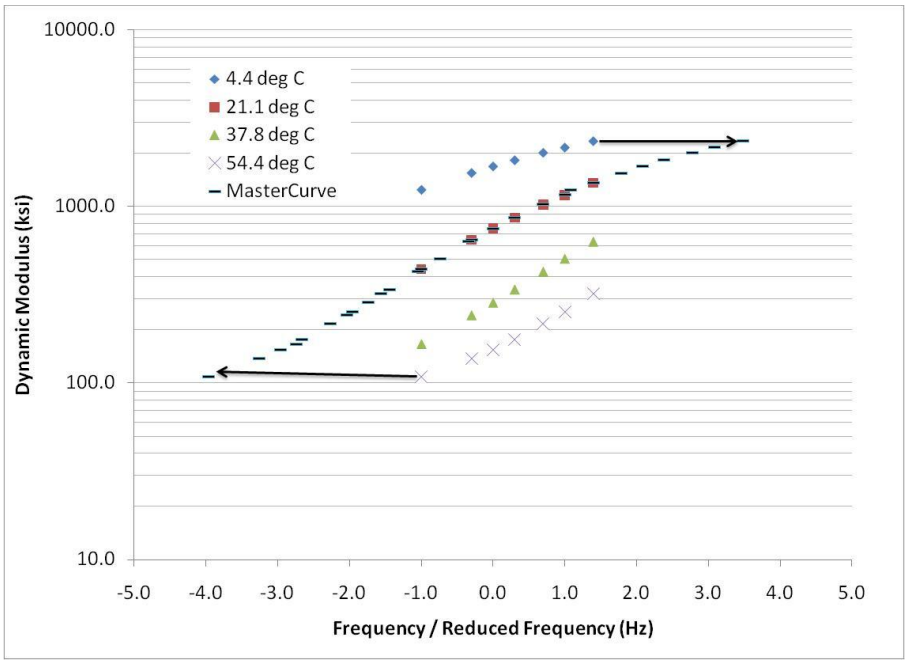

Figure 10 Use of Time-Temperature Shift Factors to Generate a Dynamic Modulus Mastercurve

Figure 11 shows the dynamic modulus mastercurves for both the WMA and HMA placed for this project. This plot shows that at the higher temperature, slower loading frequency portion of the curve (left-hand portion) the WMA was approximately 15 ksi softer than the HMA. However, as the temperature decreases and the rate of loading increases (increased reduced frequency – moving to the right-hand portion of the curve) the WMA stiffness is comparable to and even exceeds that of the HMA for the majority of the reduced frequencies plotted. Therefore, there was not a clear separation in the stiffness of the two mixes and the WMA was not clearly softer than the HMA in the dynamic modulus test. The raw test data and the master curve coefficients are given in APPENDIX D.

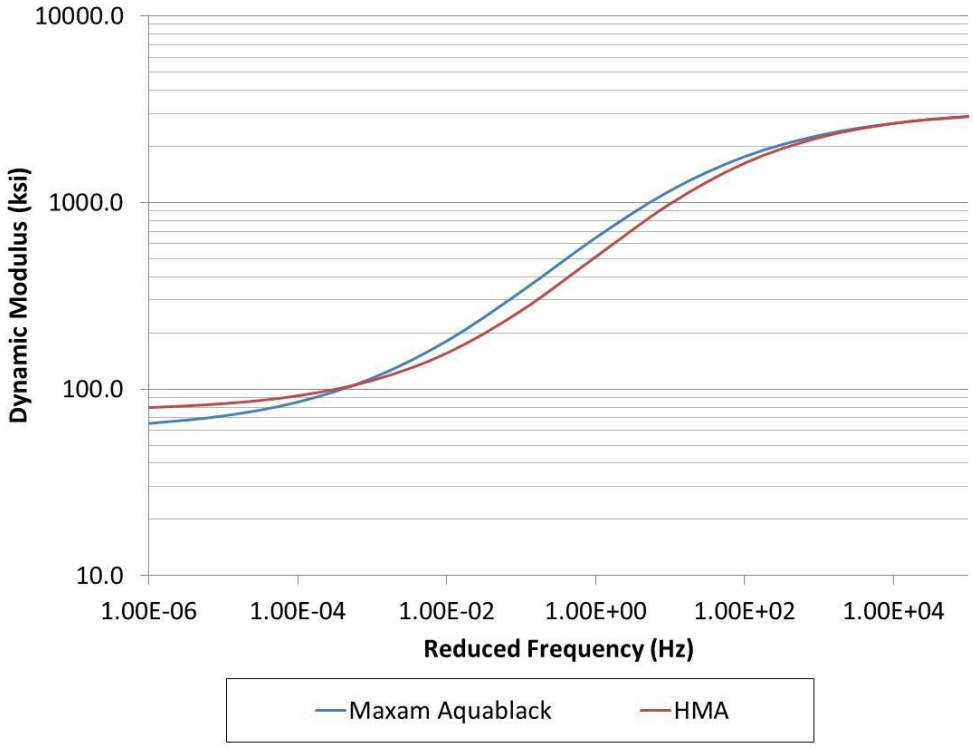

Figure 11 Dynamic Modulus Master Curves – Walla Walla, WA

7.2 Moisture-Susceptibility Testing

AASHTO T 283-07, *Resistance of Compacted Hot Mix Asphalt (HMA) to Moisture-Induced Damage*, is a moisture-susceptibility test based on evaluating the change in tensile strength between dry and moisture-saturated specimens. The test is the most common moisture-susceptibility test used by state agencies (*3*). The standard acceptance criterion is a tensile-strength ratio that equals or exceeds 80 percent per AASHTO M 323.

Specimens were compacted in the NCAT mobile laboratory from plant-produced mix without reheating the mix. The target compaction dimensions were 6 in. (150 mm) in diameter and 3.75 ± 0.2 in. (95 ± 5 mm) tall. The target air-void content was 7 ± 0.5%. Specimens were grouped to result in two sets of three specimens with similar average air voids. One set of specimens was conditioned, which encompassed saturating, freezing, and thawing specimens. The conditioned samples were vacuum saturated so that the internal voids were between 70 and 80% filled with water and subjected to one laboratory freeze-thaw cycle. Both conditioned and unconditioned specimens were at the test temperature of 77±1°F (25 ± 0.5°C) prior to testing. After conditioning, specimens were loaded diametrically at a rate of 2 in./min. (50 mm/min.). The maximum compressive strength was recorded, and then the indirect tensile strength and tensile-strength ratios were calculated. Table 6 and Figure 12 summarize the results of the moisture susceptibility testing conducted in accordance with AASHTO T 283. The whiskers in Figure 12 represent plus and minus one standard deviation. All but one of the individual tensile strengths exceeded 100 psi, which is a favorable result. The tensile strengths of the WMA tended to be less than the strengths of the HMA, which is typical for WMA results. The ratio of the average tensile strengths of the conditioned

specimens to the average tensile strengths of the unconditioned specimens is defined as the tensile strength ratio (TSR). The TSR value for the WMA was 0.86, and the TSR for the HMA was 0.89. Both the HMA and WMA yielded TSR values that exceeded the AASHTO R 35 criterion of 0.8.

Table 6 AASHTO T 283 Results

Mix	Conditioned	Saturation,%	Air Voids, %	Tensile Strength (psi)	TSR
WMA	Yes	71.1	6.6	96.6	0.86
		70.1	6.8	106.7	
		78.0	7.2	102.4	
	No	0.0	6.7	121.2	
		0.0	6.9	119.7	
		0.0	6.9	115.4	
HMA	Yes	70.1	6.9	102.4	0.89
		71.6	6.6	129.8	
		72.6	6.9	126.9	
	No	0.0	6.9	138.5	
		0.0	6.5	132.7	
		0.0	7.0	134.2	

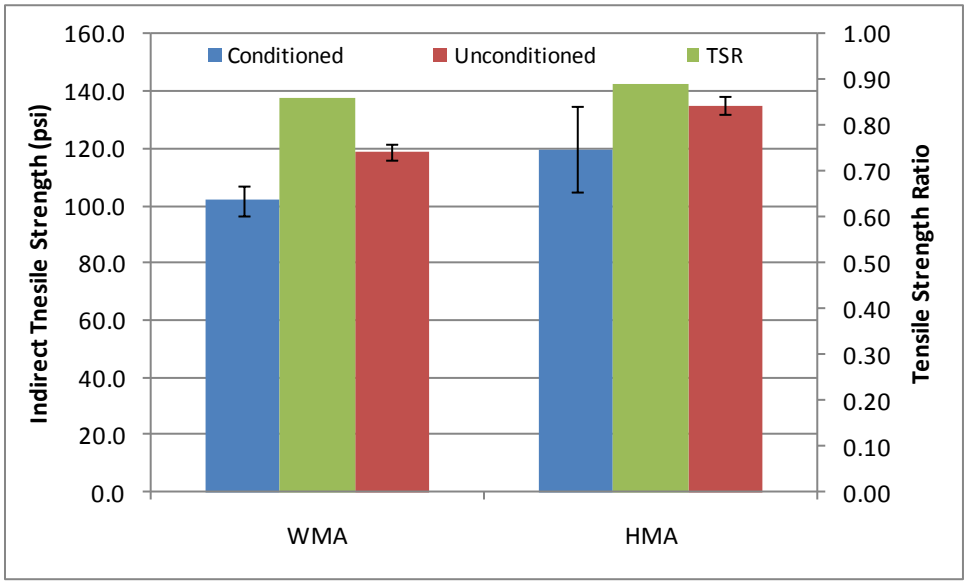

Figure 12 Moisture-Susceptibility Results.

7.3 Hamburg Wheel-Tracking Testing

AASHTO T 324-04, *Hamburg Wheel-Track Testing of Compacted Hot Mix Asphalt (HMA)*, is a loaded wheel test used to evaluate the stripping and rutting potential of a mix. Some state agencies and researchers use this test in lieu of, or in conjunction with, AASHTO T 283 to evaluate moisture susceptibility. The test employs the Hamburg Wheel-Tracking device, and specimens are typically tested in a heated water bath. For

this study, specimens were compacted to 6 in. (150 mm) in diameter by 3.75 in. (95 mm) tall in the NCAT mobile lab without reheating. The target air-void content was 7 ± 0.5%. Specimens were cut horizontally to yield two 1.875-inch (47.6 mm) thick specimens. Approximately 0.5 inch (12.7 mm) was cut vertically from one side of each specimen (see Figure 13). Two specimens were placed in a mold at once with the cut vertical sides abutting one another. The mold with the specimens was conditioned in a 122°F (50°C) water bath. Specimens were then subjected to a loaded wheel traversing the length of the two specimens. Three values for each mix were determined from the testing: stripping inflection point, rutting rate, and total rutting at 10,000 cycles (20,000 passes). The acceptable stripping inflection point criterion was a value equal to or greater than 5,000 cycles (10,000 passes). The acceptable total rut depth at 10,000 cycles (20,000 passes) was less than 0.4 in. (10 mm). A criterion for rutting rate does not exist, and the value was only used for comparing the two mixes.

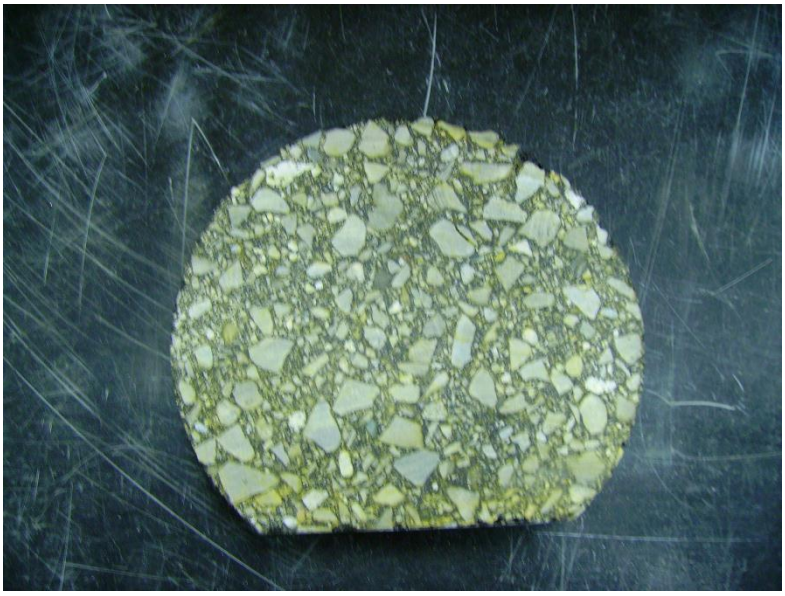

Figure 13 Cut Hamburg Specimen

The stripping inflection point, rutting rate, and total rut depth were determined for each mix. Each data point was generated from two replicate samples. Six specimens per mix were tested (two at a time) in the Hamburg Wheel-Tracking device.

Table 7 summarizes the results of the Hamburg testing.

Table 7 Hamburg Wheel-Tracking Results

Mix	Air Voids of Cut Sample (%)	Rutting Rate (mm/hr)	Total Rut Depth (mm) (Based on Rate)	Stripping Inflection Point (cycles)
WMA	6.6	2.969	11.8	9000
	7.4			
	6.8	2.283	9.1	8100
	6.5			
	5.7	1.315	5.2	7400
	5.9			
HMA	7.0	1.709	6.8	5700
	7.5			
	7.1	0.741	2.9	5800
	6.7			
	7.1	3.170	12.6	5800
	7.4			

The rutting rates were determined for both the WMA and HMA (see Table 7) and are illustrated in Figure 14. The average rutting rate of the WMA was higher than that of the HMA; however, the variability of the HMA rutting rate was greater than that of the WMA. A *t*-test indicated that the mean rutting rates were not statistically different at a level of significance of 0.05.

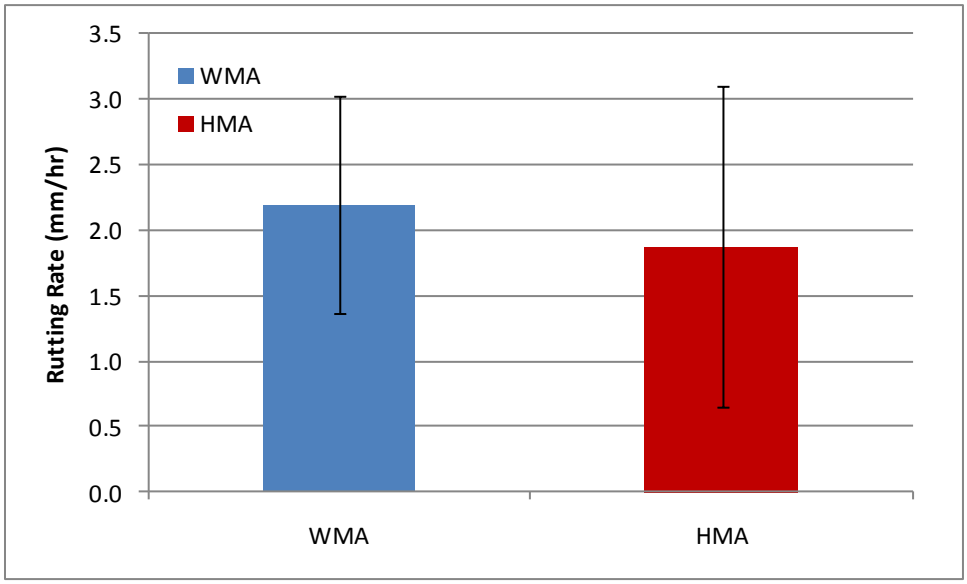

Figure 14 Hamburg Rutting Rate

The total rut depths of the WMA and HMA are illustrated in Figure 15. The WMA rut depth was greater than the HMA rut depth; however, both were less than 10 mm.

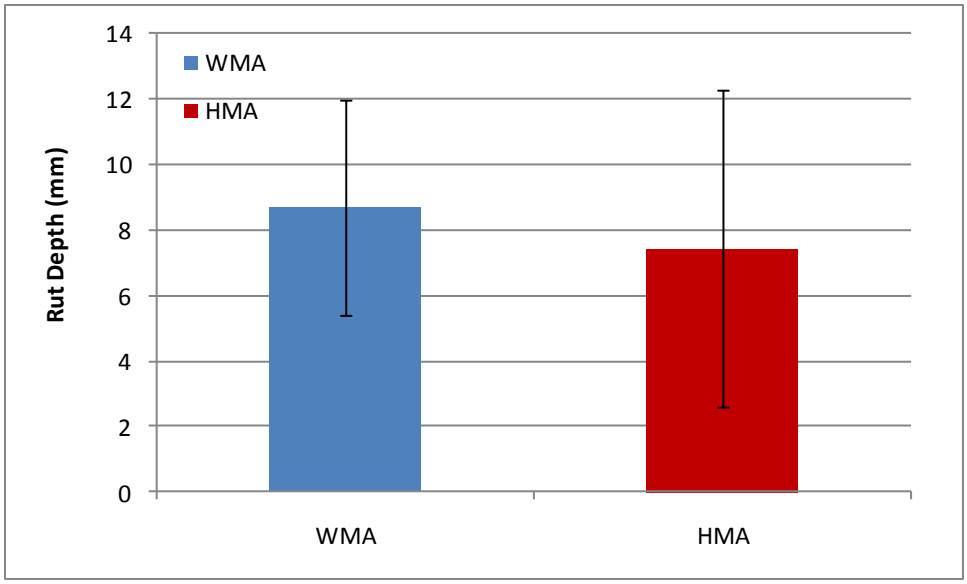

Figure 15 Hamburg Rut Depth

The stripping inflection points were determined from the test results based on the procedure outlined in AASHTO T 324. The average stripping inflection points of the mixes are displayed in Figure 16. A stripping inflection point of 5,000 cycles (10,000 passes) or more was considered acceptable. The average stripping inflection point of the WMA was greater than that of the HMA. The HMA showed higher moisture susceptibility than the WMA, though the HMA still exceeded the minimum acceptable stripping inflection point for moisture resistance during the Hamburg Wheel-Track testing.

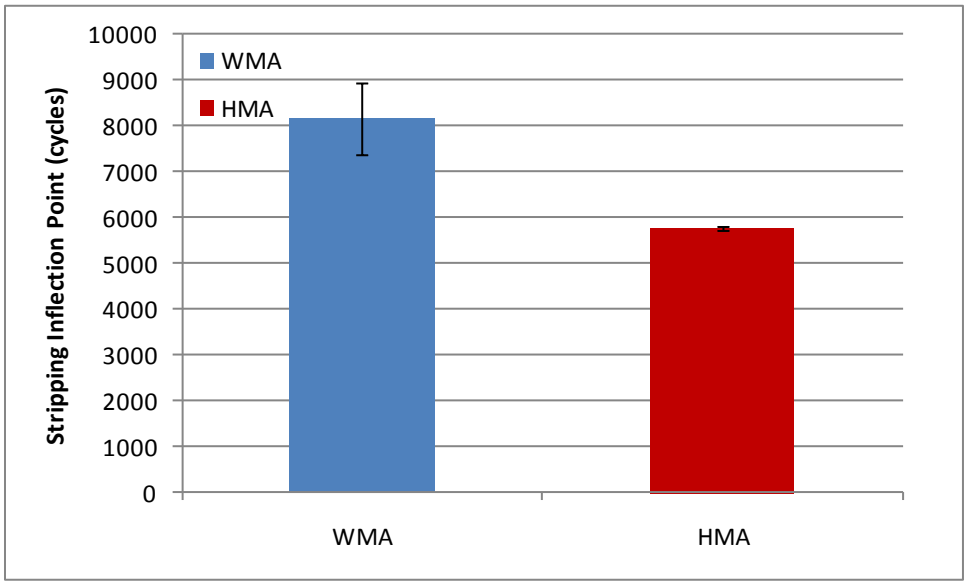

Figure 16 Hamburg Stripping Inflection Point Results

7.4 Beam Fatigue

Bending beam fatigue testing was performed in accordance with AASHTO T 321-07 to determine the fatigue limits of the WMA and HMA. Six beam specimens were tested for each mix. Within each set of six, three beams each were tested in a controlled-strain mode with target strain levels 300 and 600 microstrain.

The specimens were originally compacted in a kneading beam compactor, shown in Figure 17, then trimmed to the dimensions of 380 ± 6 mm in length, 63 ± 2 mm in width, and 50 ± 2 mm in height. The beams were compacted to a target air void level of 7 ± 1.0 percent. Additionally, the orientation in which the beams were compacted (top and bottom) was marked and maintained for the fatigue testing as well. The samples were compacted from re-heated plant-produced mix at the main NCAT laboratory (the NCAT mobile lab is not equipped with a kneading wheel compactor).

The beam fatigue apparatus, shown in Figure 17, applies haversine loading at a frequency of 10 Hz. During each cycle, a constant level of strain is applied to the bottom of the specimen. The loading device consists of 4-point loading and reaction positions that allow for the application of the target strain to the bottom of the test specimen. Testing was performed at 20 ± 0.5°C. Data-acquisition software was used to record load cycles, applied loads, strain levels, and beam deflections. Based on the dimensions of the beam and the collected data, the software calculates the stiffness of the beam after each loading iteration. At the beginning of each test, the initial beam stiffness was calculated by the data-acquisition software after 50 conditioning cycles. AASHTO T 321-07 was used to define beam failure as a 50% reduction in beam stiffness in terms of number of cycles until failure.

Figure 17 Kneading Beam Compactor (left) and IPC Global® Beam Fatigue Testing Apparatus (right)

Using a proposed procedure developed under NCHRP 9-38 (Prowell et al., 2010), the endurance limit for each mix was estimated using Equation (1) based on a 95% lower prediction limit of a linear relationship between the log-log transformation of the strain

levels (300 and 600 microstrain) and cycles to failure. All the calculations were conducted using a spreadsheet developed under NCHRP 9-38.

$$\text{Endurance Limit} = \hat{y}_0 - t_\alpha s\sqrt{1+\frac{1}{n}+\frac{(x_0-\bar{x})^2}{S_{xx}}} \quad (1)$$

where:

$\hat{y}_o$ = log of the predicted strain level (microstrain)

t_α = value of *t* distribution for n-2 degrees of freedom = 2.131847 for n = 6 with $\alpha = 0.05$

s = standard error from the regression analysis

n = number of samples = 6

S_{xx} = $\sum_{i=1}^{n}(x_i-\bar{x})^2$ (Note: log of fatigue lives)

x_o = log (50,000,000) = 7.69897

$\bar{x}$ = log of average of the fatigue life results

A summary of the bending beam fatigue test results for the WMA and HMA is provided in Table 8. Figure 18 compares the fatigue cracking resistance of the two mixtures determined based on AASHTO T 321-07 results. A power model transfer function ($\varepsilon = \alpha_1 N^{\alpha_2}$) was used to fit the results for each mixture. A summary of the model coefficients and R^2 values is given in Table 9. Additionally, a summary of the fatigue endurance limits is given in Table 9.

Visual inspection of the fatigue resistance curves in Figure 18 shows little visual difference in the fatigue resistance of the WMA and the HMA. To compare the data statistically, a two-sample *t*-test ($\alpha = 0.05$) was performed to compare the WMA and HMA cycles to failure at the different strain levels. The reslts showed no statistical difference between the WMA and HMA fatigue lives in the beam fatigue test at either 300 microstrain (*p*-value = 0.24) or 600 microstrain (*p*-value = 0.31). The R^2 values for each of the mixes are above 0.987, showing a good model fit for the dataset.

Comparing the fatigue endurance limits of the WMA and HMA (Table 9) shows the WMA had a higher fatigue endurance limit than the HMA by approximately 24 microstrain. Physically, this indicates that the WMA can endure a higher strain level than the HMA without accruing permanent damage. Therefore, the bending beam fatigue results indicate that the WMA should have equal or better fatigue performance in comparison to the control HMA.

Table 8 Bending Beam Fatigue Results

Mix	Microstrain Level	Beam ID	Number of Cycles to Failure
WMA	600	W3	9,420
WMA	600	W5	9,560
WMA	600	W6	12,730
WMA	300	H57	411,050
WMA	300	H58	637,530
WMA	300	H59	420,910
HMA	600	H51	11,600
HMA	600	H52	11,140
HMA	600	H53	13,560
HMA	300	W7	451,280
HMA	300	W8	378,610
HMA	300	W9	241,410

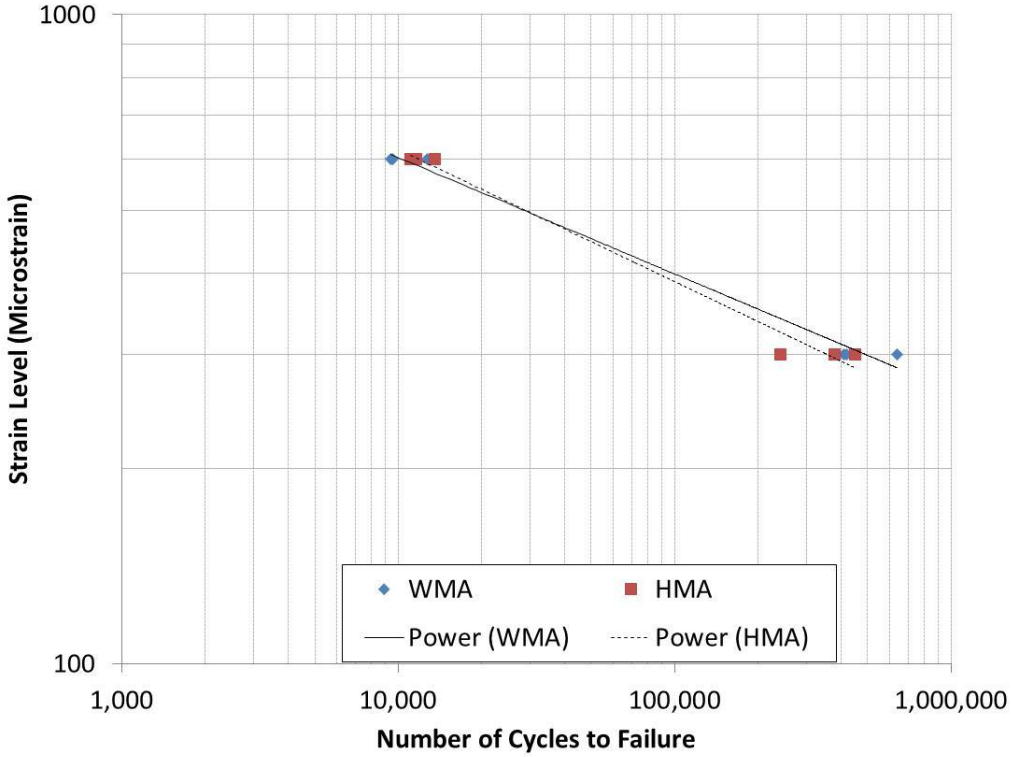

Figure 18 Fatigue Resistance Curves

Table 9 Fatigue Curve Fitting Coefficients (Power Model) and Endurance Limit

Mixture	α_1	α_2	R^2	Fatigue Endurance Limit (microstrain)
WMA	3158.7	-0.18	0.9919	113
HMA	4053.9	-0.204	0.9866	89

7.5 Thermal Cracking

In thermal cracking analysis, the temperature at which the estimated thermal stress in a pavement due to contraction exceeds the tested indirect tensile strength of a mixture is used to assess low-temperature cracking performance of asphalt mixtures. This type of analysis is referred to as a "critical temperature analysis." A mixture exhibiting a lower critical cracking temperature than those of the other mixtures would have better resistance to thermal cracking. Both the WMA and HMA mixtures were evaluated using a critical temperature analysis for this study. To estimate the thermal stress and measure the tensile strength at failure, the indirect tensile creep compliance and strength tests were conducted as specified in AASHTO T 322-07, *Standard Method of Test for Determining the Creep Compliance and Strength of Hot-Mix Asphalt (HMA) Using the Indirect Tensile Test Device*. A thermal coefficient of each mixture was estimated based on its volumetric properties and typical values for the thermal coefficient of asphalt and aggregate. This computation is explained in more detail below.

The testing was conducted using an indirect tensile testing (IDT) system with an MTS® load frame and an environmental chamber capable of maintaining the temperatures required for this test. Creep compliances at 0◦C, -10◦C, and -20◦C and tensile strength at -10◦C were measured in accordance with AASHTO T 322-07. These temperatures are specified as a function of the low-temperature PG grade of the binder in AASHTO T322-07. The creep test applies a constant load to the asphalt specimen for 100 seconds while the horizontal and vertical strains are measured on each face of the specimen using on-specimen instrumentation.

Four specimens were prepared for each mix from hot-compacted plant-produced mix. The first specimen was used to find a suitable creep load for that particular mix at each testing temperature. The remaining three specimens were tested at this load for data analysis. Specimens used for the creep and strength tests were 38 to 50 mm thick and 150 mm in diameter. Specimens were prepared to 7 ± 0.5% air voids. Figure 19 shows a photo of the MTS load frame and the load guide device used for IDT testing.

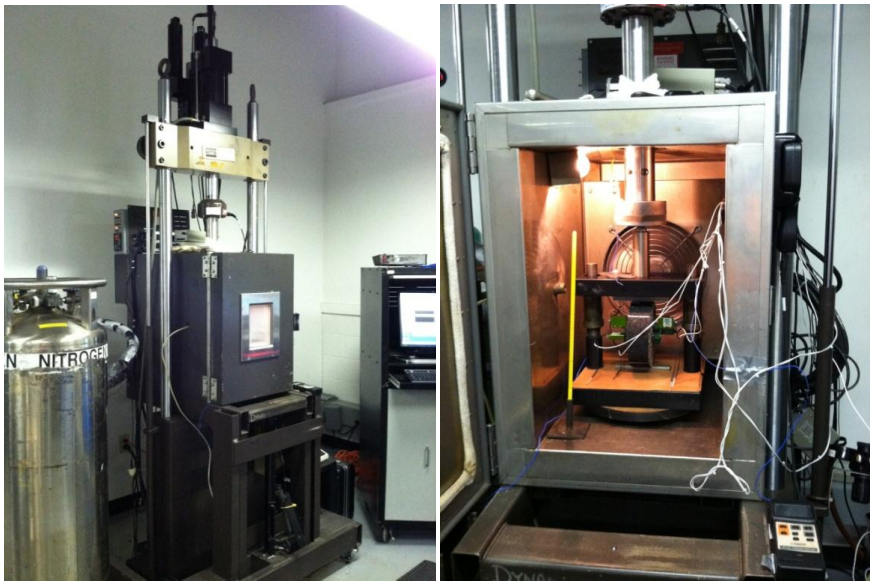

Figure 19 MTS® Load Frame (left) and Specimen Setup for IDT Testing (right)

For linear visco-elastic materials, the effect of time and temperature can be combined into a single parameter through the use of the time-temperature superposition principle (similarly to the dynamic modulus data discussed previously). From a proper set of creep compliance tests under different temperature levels, the creep compliance mastercurve can be generated by shifting the creep compliance data to a curve based on a reference temperature. This reference temperature is typically the lowest creep compliance test temperature (-20◦C for this study). The relationship between real time *t*, reduced time ξ, and a shifting factor a_T are given as Equation (2).

$$\xi = t/a_T \qquad (2)$$

An automated procedure to generate the mastercurve was developed as part of the Strategic Highway Research Program (SHRP) (Buttlar et al, 1998). The system requires the measurement of creep compliance test data at three different test temperatures. The creep compliance data used for this generation of the creep compliance mastercurve are listed in APPENDIX D. The final products of the system are a generalized Maxwell model (or Prony series), which is several Maxwell elements connected in parallel, and temperature shifting factors. The generalized Maxwell model and shifting factors are used for predicting thermal stress development of the asphalt mixture due to change in temperature. The Maxwell model elements and shift factors generated through the analysis system for this project are listed in APPENDIX D.

In addition to thermo-mechanical properties, it is required to estimate the thermal coefficient of the asphalt mixture for the critical temperature analysis. The linear thermal coefficients, α, of the given asphalt mixtures were estimated using the relationship below, which is a modified version of the relationship proposed by Jones et al. (1968) (Equation [3]). The estimated thermal coefficients were 2.042×10^{-5} ($1/^{o}C$) for the WMA and 2.053×10^{-5} ($1/^{o}C$) for the HMA.

$$\alpha_{MIX} = \frac{VMA * BAC + V AGG * BAGG}{3 * VTOTAL} \quad (3)$$

Where: α_{MIX} = linear coefficient of thermal contraction of the asphalt mixture (1/°C)
B_{AC} = volumetric coefficient of thermal contraction of the asphalt cement in the solid state (3.45 x 10^{-4}/°C)
B_{AGG} = volumetric coefficient of thermal contraction of the aggregate (1x10^{-6}/°C)
VMA = percent volume of voids in the mineral aggregate
V_{AGG} = percent volume of aggregate in the mixture
V_{TOTAL} = 100 percent

Based on the above parameters, the change in thermal stress for each mixture was estimated at the cooling rate of 10°C per hour starting at 20°C. The finite difference solution below developed by Soules et al. (1987) was used to estimate thermal stress development based on the Prony Series coefficients (Equations 4 and 5). This analysis was performed in a MATHCAD program developed at NCAT.

$$\sigma_i(t) = e^{-\Delta\xi/\lambda_i}\sigma_i(t - \Delta t) + \Delta\varepsilon E_i \frac{\lambda_i}{\Delta\xi}\left(1 - e^{-\Delta\xi/\lambda_i}\right) \quad (4)$$

$$\sigma(t) = \sum_{i=1}^{N+1}\sigma_i(t) \quad (5)$$

Where:

σ = thermal stress
ΔT and $\Delta\xi$ = changes in temperature and reduced time over the small time Δt

A complete description of the thermal stress analysis can be found in Hiltunen and Roque (1992) and Kim et al. (2008). Figure 20 shows thermal stress development as a function of a reduction in temperature. This data shows the HMA to accrue thermal stress at a higher rate than the WMA when pavement temperatures drop below -20°C. Recall that the "critical" temperature is the temperature at which the predicted stresses exceed the measured tensile stress. For the WMA, this temperature is -25.6°C and for the HMA, this temperature is -25.0°C. Practically speaking, the WMA and HMA perform equally in terms of resistance to thermal cracking.

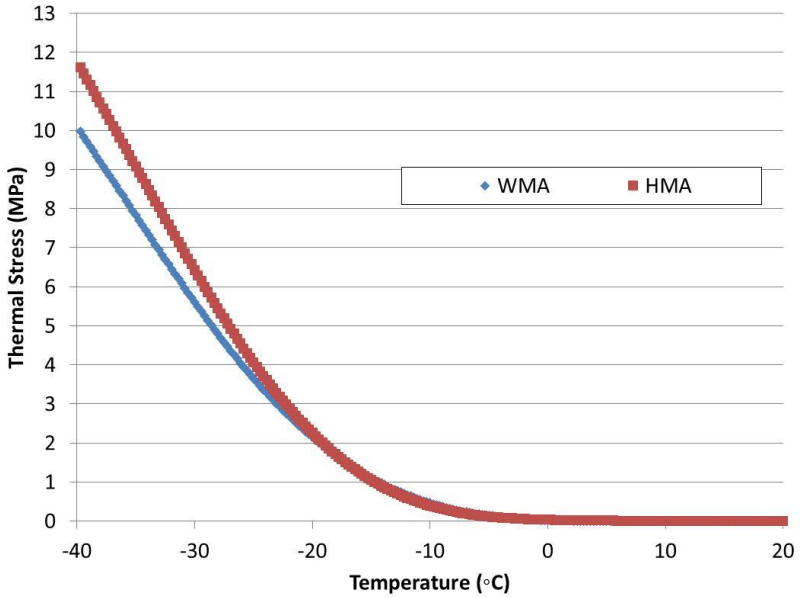

Figure 20 Thermal Stress Development as a Function of Temperature – IDT Specimens

The critical cracking temperatures were also compared with the 98% reliability low-temperature grade for the Walla Walla, WA area in LTPPBind v3.1. This temperature was determined at the surface of the pavement with no adjustments for traffic (worst-case scenario). This 98% reliability low temperature was found to be -23.9°C for the Walla Walla area. The critical temperature for both the WMA and HMA fall below this temperature. Therefore, neither the WMA nor HMA should have an issue with thermal cracking in the field. Given the virgin binder for this mix was a PG 64-28, the results from the critical temperature analysis are reasonable.

7.6 Flow Number

The flow number test is a rutting resistance test that is performed using the Asphalt Mixture Performance Tester (AMPT). It applies a repeated compressive loading to an asphalt specimen while the AMPT records the deformation of the specimen with each loading cycle. The user defines the temperature, applied stress state (deviator stress and confining stress), and number of cycles at which the test is performed. The loading is applied for 0.1 seconds followed by a 0.9 second rest period every 1 second cycle. Flow number data is commonly modeled with the Francken model (Biligiri et al, 2007), shown as Equation 4. An example of flow number test data is shown as Figure 21.

$$\varepsilon_p(N) = aN^b + c(e^{dN} - 1) \qquad (6)$$

Where: ε_p = Permanent Strain
a,b,c,d = Regression Coefficients
N = Number of Testing Cycles

The flow number is defined as the number of cycles at which the sample begins to rapidly deform. This is more properly defined as the breakpoint between steady-state rutting (secondary rutting) and the more rapid failure of the specimen (tertiary flow).

Figure 21 demonstrates this concept graphically. A higher flow number (or less permanent deformation for confined samples) is indicative of a mixture with greater resistance to rutting in the field.

If the samples do not exhibit tertiary flow (which is common for confined samples), then the amount of deformation at a specified loading cycle can still be used to give a relative ranking of tested mixes with respect to rutting susceptibility. An example of the typical behavior for a confined flow sample is shown in Figure 22.

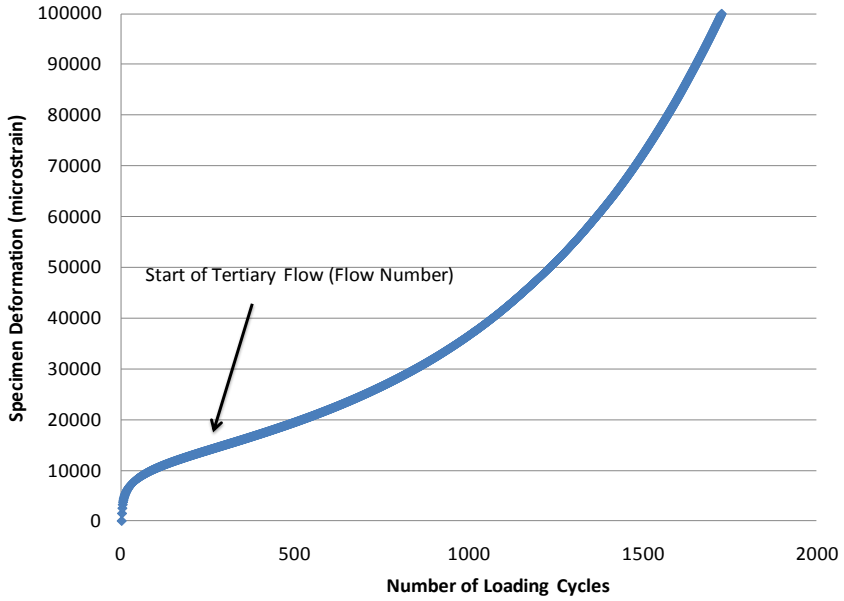

Figure 21 Typical Unconfined Flow Number Test Data

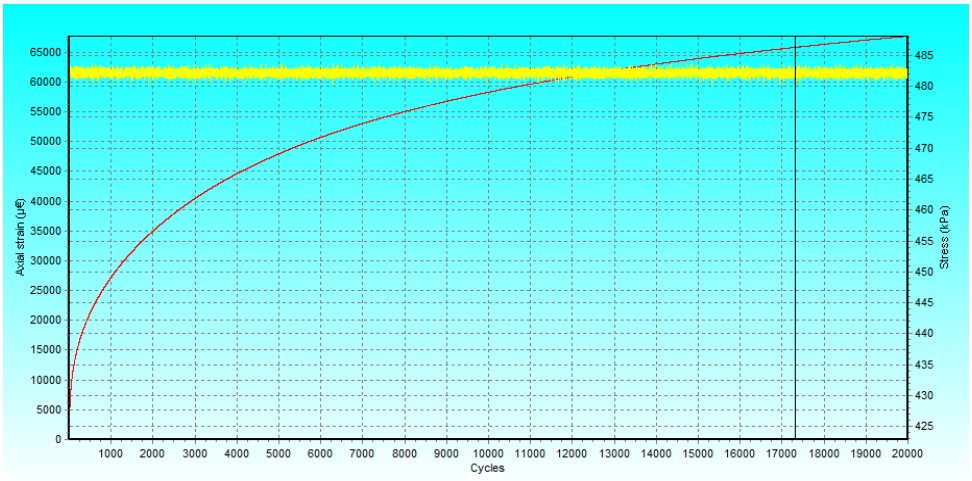

Figure 22 Common Behavior for Confined Flow Test

Flow number testing for this project was performed in accordance with AASHTO PP79-09. Test specimens were prepared in accordance with AASHTO PP61-09 to a target air void level of 7 ± 0.5%. Three specimens per mix were tested. AASHTO TP 79-09 does not specify whether to test the specimens confined or unconfined. For research purposes, a set of samples for each mix were tested confined and a set were tested unconfined. The confined specimens were compacted from plant-produced mix re-heated in the NCAT laboratory. Two sets of unconfined specimens were available. A limited number of AMPT samples compacted in the field (at the NCAT mobile lab) were available in addition to samples that were re-heated for compaction at the NCAT main lab. Therefore, the samples were available to perform a mini-comparison study on whether the presence of the re-heating process had any impact on the performance of the mixture in the flow number test.

One set of flow number specimens was tested in accordance with the recommendations from NCHRP 09-43. Specimens were tested unconfined (0 psi) using a deviator stress of 87 psi. The target testing temperature was 53°C, which is the LTPP 50% reliability high temperature for Walla Walla, WA adjusted to a depth of 20 mm in the pavement structure.

The confined sets of specimens were tested using a confining pressure of 10 psi and a deviator stress of 100 psi. The testing temperature was 53°C. Each confined flow number test ran the full 20,000 cycles before being terminated by the software. To determine the relative deformation resistance of these mixes, two parameters were measured. First, the permanent deformation of each sample after 20,000 loading cycles was recorded. Secondly, the slope of the steady-state portion of the rutting curve (after initial consolidation) was calculated. For consistency, this was calculated as the slope of the sample deformation between cycle 10,000 and cycle 20,000.

Figure 23 shows a boxplot of the unconfined flow number test results. A Tukey-Kramer test ($\alpha = 0.05$) was performed to assess statistical differences. These comparisons are summarized in
Table 10. A complete listing of the *p*-values from the Tukey-Kramer test along with all of the individual unconfined flow number results are given in APPENDIX D. While the average flow number values for the re-heated mixes were higher than those compacted in the field lab, the statistical analysis indicates that the results were not statistically different results for either the WMA or HMA. The statistical analysis also indicates that for the lab-reheated samples, the HMA had a statistically higher flow number than the WMA, indicating the HMA would be more resistant to rutting than the WMA. However, for the field-compacted samples, the flow number results for WMA and HMA were not statistically different.

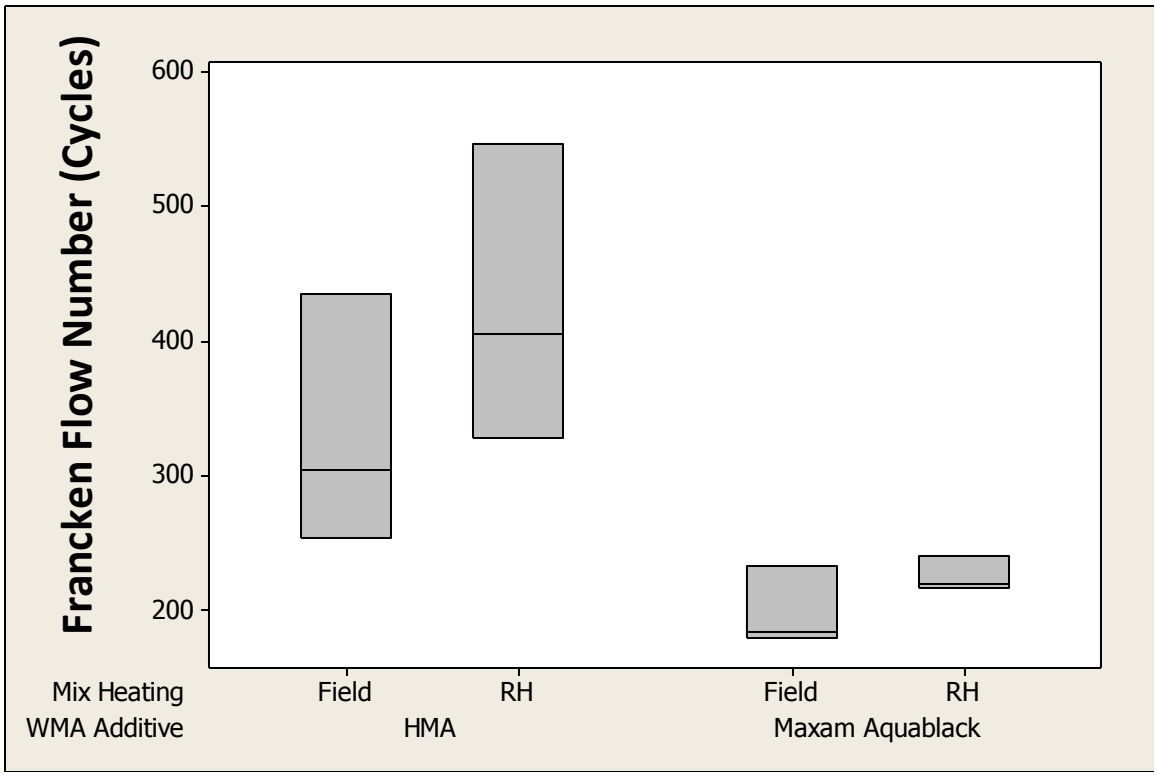

Figure 23 Boxplot of Flow Number Results

Table 10 Tukey-Kramer (α = 0.05) Statistical Groupings for Flow Number Test Results

WMA Additive	Mix Heating	Mean Flow Number	Tukey-Kramer Statistical Grouping
HMA (none)	Lab Re-heated	426.3	A
HMA (none)	Field-Compacted	331.7	A , B
Maxam Aquablack	Lab Re-heated	226.7	B
Maxam Aquablack	Field-Compacted	199.7	B

Table 11 shows the statistical comparisons of the confined flow number data for this project using an ANOVA (α = 0.05). The data shows no evidence of a statistical difference between the WMA and HMA for comparisons between accumulated microstrain at 20,000 testing cycles or for the slope of the steady-state portion of the deformation versus cycles curves. Recall that these samples were fabricated in the laboratory from re-heated plant-produced mix. The statistical comparisons from the confined flow number testing do not agree with those from the unconfined flow number testing. The complete data set for the unconfined flow number test can be found in APPENDIX D.

Considering all of the flow number results, the evidence is not conclusive with regard to the relative potential for rutting of WMA compared to HMA. This finding is consistent with the results of the Hamburg testing.

Table 11 Statistical Comparison of Confined Flow Number Test Data

WMA Additive	WMA	HMA
Average Microstrain at 20,000 cycles	47219	45020
Standard Deviation of Microstrain at 20,000 Cycles	4202.0	2222.6
ANOVA p-value vs. HMA ($\alpha = 0.05$)	0.468	
Average Steady-State Rutting Slope	0.688	0.670
Standard Deviation of Steady-State Rutting Slope	0.071	0.059
ANOVA p-value vs. HMA ($\alpha = 0.05$)	0.759	

8. ONE-YEAR PROJECT REVISIT

A field-performance evaluation was conducted on May 17, 2011, after about 13 months of traffic were applied to the test sections. Data were collected on each section to document performance regarding rutting, cracking, and raveling. This was done by randomly selecting three 200-foot (61-m) "data sections" within each mix section. Also, for both the HMA and WMA, three 6-inch (150-mm) diameter cores were taken from the outside wheelpath, and four 6-inch (150-mm) diameter cores were taken from in between the wheelpath. These cores were used to determine the in-place density after 13 months, indirect tensile strengths, theoretical maximum specific gravity, gradation, asphalt content, and the true binder grade for each mix.

Rutting

The rut depths were measured at the beginning of each 200-foot "data section" with a string line. Neither the HMA or WMA showed significant rutting after 13 months, with the HMA having an average rut depth of 0.99-mm, and the WMA having no measurable rut depth.

Cracking

Each 200-foot section was carefully inspected for visual signs of cracking. No cracking was evident in any of the HMA or WMA sections.

Raveling and Weathering

The surface textures of both the HMA and WMA test sections were measured using the sand patch test according to ASTM E965. The sand patch test was conducted at the beginning of each 200-foot section in the outside wheelpath. The calculated mean texture depths for each mix are shown in TABLE 12. These values represent the average and standard deviation of the three tests conducted on each mix. A smaller mean texture depth indicates a smoother pavement, or one with less surface texture.

TABLE 12 Mean Texture Depths

Mix	Mean Texture Depth (mm)	Standard Deviation
HMA	1.00	0.13
WMA	0.74	0.05

These results show that the HMA has a higher mean texture depth, which indicates that the HMA has raveled more than the WMA. The difference in textures is likely due to the HMA being placed in the travel lane while the WMA was placed in the passing lane. As shown in FIGURES 24-26, the raveling is visually apparent. Based on the author's experience, it is not clear if this amount of raveling is typical of pavements in this region of the country. The raveling is greater than what is typical of coarse-graded pavements after one year of traffic in the milder climates of the southeast U.S.

Figure 24 WMA (Foreground) and HMA (Background) Sections

Figure 25 HMA Surface Texture

Figure 26 WMA Surface Texture

Core Testing

At the time of the one-year project inspection, seven 6-inch (150-mm) cores were taken from each mix section. Four of these cores came from between the wheelpaths, and three

came from the outside wheelpath. These cores were all taken from one general location near the construction cores. These densities of these cores were measured using AASHTO T 166. Six of the cores were then tested for tensile strength using ASTM D6931. These six samples were then combined and the cut-faces were removed. This mix was split into two samples that were used to determine the maximum specific gravity according to AASHTO T 209. These same two samples were then dried and extracted according to AASHTO T 164. The extracted binder was graded according to AASHTO R 29. A summary of the core testing is shown in Table 13, and the complete results are shown in Appendix C.

The one-year revisit cores showed slightly lower air voids compared to the construction cores, as expected due to densification under the applied traffic load. The HMA cores exhibited lower average air voids (4.1%) than the WMA cores (4.8%). This is probably because the HMA has been subjected to slightly more traffic since it was placed in the travel lane, and the WMA was placed in the passing lane. The gradations were very similar for the HMA and WMA, and had not changed significantly from the cores taken at construction. The asphalt contents for the HMA and WMA one-year cores were more similar than were the construction cores. The HMA asphalt content (5.88%) was very close to the asphalt content of the construction cores (5.69%). The WMA asphalt content (5.78%) was significantly higher than that of the construction cores (4.87%) but was closer to the asphalt content from the plant mix sampled during construction (5.11%). These differences can probably be attributed to construction variability. In addition, the asphalt content from the construction cores was taken from only one sample since that was all the material that was available from the five 4-inch diameter construction cores, while the one-year revisit asphalt content was an average value taken from two samples.

The tensile strengths of the one-year cores were less than the strengths of the construction cores, but the tensile strengths for both the HMA and WMA were similar and reasonable. The extracted binder grades for the HMA and WMA were very similar and had not changed significantly from the binder grade of the construction cores.

Table 13 Test Results on Construction and One-Year Cores

	HMA	**WMA**	**HMA**	**WMA**
	Construction Cores (April 2010)		**1 Year Revisit Cores (May 2011)**	
Sieve Size	**% Passing**		**% Passing**	
25.0 mm (1”)	100.0	100.0	100.0	100.0
19.0 mm (3/4”)	100.0	100.0	100.0	100.0
12.5 mm (1/2”)	96.6	94.1	95.4	94.1
9.5 mm (3/8”)	84.5	82.5	81.9	80.6
4.75 mm (#4)	56.3	54.5	51.9	52.8
2.36 mm (#8)	37.4	37.2	34.5	36.5
1.18 mm (#16)	27.2	27.5	25.2	27.4
0.60 mm (#30)	21.2	21.8	19.8	21.9
0.30 mm (#50)	17.5	18.1	16.5	18.4

0.15 mm (#100)	11.5	11.8	11.4	12.5
0.075 mm (#200)	7.3	7.3	7.7	8.2
Asphalt Content (%)	5.69	4.87	5.88	5.78
G_{mm}	2.598	2.606	2.613	2.617
G_{mb}	2.459	2.459	2.506	2.490
V_a (%)	5.4	5.6	4.1	4.8
P_{ba} (%)	1.04	0.62	1.40	1.40
Tensile Strength (psi)	160.9	165.4	104.9	120.4
Recovered Binder True Grade	72.9+22.2-26.1	75.7+19.2-25.9	73.7+22.4-27.2	74.7+21.6-27.3

Table 14 shows the average air void and tensile strength results by location for the one-year revisit cores. The air voids were lower in the wheelpaths as compared to those between the wheelpaths for both the HMA and WMA, as expected. Also, the tensile strengths for both mixes were slightly lower in the wheelpaths than those between the wheelpaths, as expected.

Table 14 Air Void and Tensile Strengths by Location

	HMA	**WMA**
	1 Year Revisit Cores	
Between Wheelpaths V_a (%)	4.3	5.1
In Outside Wheelpath V_a (%)	3.8	4.6
Between Wheelpaths Tensile Strength (psi)	114.6	126.4
In Outside Wheelpath Tensile Strength (psi)	95.3	114.3

9. SUMMARY OF FINDINGS

In April 2010, a WMA field evaluation was constructed in Walla Walla, WA, to compare conventional HMA with WMA produced using the AquaBlack™ asphalt foaming system developed by Maxam Equipment. Findings from this evaluation include the following:

- The WMA production temperature was approximately 50°F less than that of the HMA.
- No problems were encountered during the construction of the WMA section.
- Laboratory test results (gradation, asphalt content, and volumetrics) on plant mix and cores were similar and satisfactory for both the WMA and HMA.
- Laboratory TSR results indicate similar performance with regard to moisture susceptibility for both the WMA and HMA.
- Hamburg Wheel-Tracking results indicate satisfactory rutting performance for both the WMA and HMA.

- The WMA and HMA exhibited similar stiffnesses across the full range of tested temperatures and frequencies in the dynamic modulus test.
- The WMA and HMA beam fatigue results were not statistically different, with the WMA having a higher fatigue endurance limit. Therefore, the WMA should have equal or better performance than the control HMA in terms of fatigue.
- The temperature at which low temperature thermal cracking will occur was calculated from creep compliance and strength testing. This testing showed the WMA and HMA had equivalent resistance to low-temperature cracking. The critical cracking temperature was also below that of the 98% reliability low pavement temperature calculated from LTPPBind v3.1. Therefore, both the WMA and HMA should have adequate resistance to thermal cracking.
- Flow number tests were performed on specimens in confined and unconfined stress states. The unconfined tests were performed on both field-compacted and lab reheated plant-produced mix. For field-compacted specimens, the analysis of the unconfined flow number data showed no statistical difference in the results for the WMA and HMA. However, for specimens compacted from reheated mix, the confined and unconfined flow number test results were not statistically different for HMA and WMA.
- After 13 months in service, the HMA and WMA sections exhibited similar field performance. Both sections have virtually no rutting or cracking, but they had an appreciable amount of raveling. Tests on cores taken from the WMA and HMA pavements had very similar characteristics.

REFERENCES

1. Hurley, G. C. and B. D. Prowell. Evaluation of Evotherm for Use in Warm Mix Asphalt. NCAT Report 06-02 (2006).
2. Washington State DOT. http://www.wsdot.wa.gov/Projects/US12/FrenchtowntoWallaWalla/. Accessed April 29, 2010.
3. Solaimanian, M., R.F. Bonaquist, and V. Tandon. Improved Conditioning and Testing Procedures for HMA Moisture Susceptibility. NCHRP Report 589 (2007).
4. Prowell, B.D., E.R. Brown, R.M. Anderson, J. Sias-Daniel, H. Von Quintus, S. Shen, S.H. Carpenter, S. Bhattacharjee and S. Maghsoodloo. *Validating the Fatigue Endurance Limit for Hot Mix Asphalt*. NCHRP Report 646, Transportation Research Board, Washington, D.C., 2010.
5. W.G. Buttlar, R. Roque, and B. Reid, "Automated Procedure for Generation of Creep Compliance Master Curve for Asphalt Mixtures," Transportation Research Record, 1630: 28-36, 1998.
6. G.M. Jones, M. I. Darter, and G. Littlefield. "Thermal Expansion-Contraction of Asphaltic Concrete," Journal of the Association of Asphalt Paving Technologists, 37, 1968: 56-97.
7. T.F. Soules, R. F. Busbey, S. M. Rekhson, A. Markovsky, and M. A. Burke. "Finite-Element Calculation of Stresses in Glass Parts Undergoing Viscous Relaxation," Journal of the American Ceramic Society, 70 (2), 1987: 90-95.
8. J. Kim, R. Roque, and B. Birgisson, "Integration of Thermal Fracture in the HMA Fracture Model," Journal of the Association of Asphalt Paving Technologists, 77, 2008: 631-662.
9. R. Roque and W.G. Buttlar. The Development of a Measurement and Analysis System to Accurately Determine Asphalt Concrete Properties Using the Indirect Tensile Mode. Journal of the Association of Asphalt Paving Technologists, Vol. 61, 1992, pp. 304-332.
10. K.P. Biligiri, K.E. Kaloush, M.W. Mamlouk, and M.W. Witczak, Rational Modeling of Tertiary Flow of Asphalt Mixtures, *Transportation Research Record: Journal of the Transportation Research Board*, No. 2001,2007, pp. 63-72.

APPENDIX A – PRODUCTION TESTING DATA

Table A1 Mix Moisture Content Data

	Moisture Content, %	
	HMA	**WMA**
Sample 1	0.06	0.22
Sample 2	0.08	0.23
Average	0.07	0.23

Note: Sampling frequency was twice per mix per day of production.

Table A2 Coating Data

	Percent of Coated Particles, %
HMA	99.3
WMA	100.0

Note: Sampling frequency was once per mix per day of production.

Table A3 Gradation and Asphalt Content—HMA Plant Mix

	% Passing					
Sieve Size	**Sample 1**		**Sample 2**		**Average**	**Std. Deviation**
25.0 mm (1")	100.0		100.0		100.0	0.0
19.0 mm (3/4")	100.0		100.0		100.0	0.0
12.5 mm (1/2")	94.8		93.2		94.0	1.1
9.5 mm (3/8")	81.3		78.8		80.1	1.8
4.75 mm (#4)	53.2		50.6		51.9	1.8
2.36 mm (#8)	34.2		32.5		33.4	1.2
1.18 mm (#16)	23.9		22.5		23.2	1.0
0.6 mm (#30)	18.2		17.1		17.6	0.8
0.3 mm (#50)	14.8		13.8		14.3	0.7
0.15 mm (#100)	9.9		9.0		9.5	0.6
0.075 mm (#200)	6.5		5.6		6.0	0.6
	Sample 1	**Sample 2**	**Sample 3**	**Sample 4**	**Average**	**Std. Deviation**
Asphalt Content, %	6.22	5.79	5.64	4.99	5.66	0.51

Table A4 Gradation and Asphalt Content—WMA Plant Mix

	% Passing				
Sieve Size	**Sample 1**	**Sample 2**	**Average**	**Std. Deviation**	
25.0 mm (1")	100.0	100.0	100.0	0.0	
19.0 mm (3/4")	100.0	100.0	100.0	0.0	
12.5 mm (1/2")	95.6	95.3	95.4	0.2	
9.5 mm (3/8")	80.0	82.0	81.0	1.4	
4.75 mm (#4)	49.4	49.7	49.5	0.3	
2.36 mm (#8)	31.2	31.4	31.3	0.1	
1.18 mm (#16)	22.1	21.7	21.9	0.3	
0.6 mm (#30)	17.1	16.6	16.8	0.3	
0.3 mm (#50)	14.1	13.6	13.8	0.4	
0.15 mm (#100)	10.2	9.2	9.7	0.7	
0.075 mm (#200)	6.9	6.2	6.6	0.5	

	Sample 1	**Sample 2**	**Sample 3**	**Sample 4**	**Average**	**Std. Deviation**
Asphalt Content, %	4.93	5.68	4.75	5.09	5.11	0.40

Table A5 Volumetric Properties—HMA Plant Mix

Sample	**Gyrations**	**Compaction Temperature, °F**	**G_{mb}**	**G_{mm}**	**V_a, %**	**Water Absorption, %**
1	100	300	2.513	2.606	3.6	0.4
2	100	300	2.521	2.606	3.2	0.5
Average			2.517		3.4	0.5

Note: G_{mm} is an average value, based on two samples (2.611 and 2.601).

Table A6 Volumetric Properties—WMA Plant Mix

Sample	**Gyrations**	**Compaction Temperature, °F**	**G_{mb}**	**G_{mm}**	**V_a, %**	**Water Absorption, %**
1	100	250	2.505	2.597	3.5	0.6
2	100	250	2.512	2.597	3.3	0.6
Average			2.509		3.4	0.6

Note: G_{mm} is an average value, based on two samples (2.593 and 2.601).

APPENDIX B – CORE TESTING DATA

Table B1 Volumetric Properties and Tensile Strength—HMA Cores

Sample	G_{mb}	G_{mm}	V_a, %	Water Absorption, %	Avg. Diameter, in.	Avg. Height, in.	Failure Load, lb.	Tensile Strength, psi
1	2.447	2.598	5.8	0.8	2.998	1.199	1100	146.1
2	2.443	2.598	6.0	0.7	4.005	1.101	1100	158.8
3	2.477	2.598	4.7	0.4	4.000	0.904	900	158.5
4	2.484	2.598	4.4	0.3	4.005	1.542	1700	175.2
5	2.445	2.598	5.9	0.7	4.000	1.391	1450	165.9
Average	**2.459**		**5.3**	**0.6**	**4.002**	**1.227**	**1250**	**160.9**

Note: G_{mm} is based on one sample.

Table B2 Volumetric Properties and Tensile Strength—WMA Cores

Sample	G_{mb}	G_{mm}	V_a, %	Water Absorption, %	Avg. Diameter, in.	Avg. Height, in.	Failure Load, lb.	Tensile Strength, psi
1	2.434	2.606	6.6	0.9	3.996	1.604	1600	158.9
2	2.453	2.606	5.9	0.6	4.009	1.529	1500	155.8
3	2.473	2.606	5.1	0.6	3.998	1.542	1700	175.6
4	2.456	2.606	5.7	0.5	4.004	1.588	1650	165.2
5	2.479	2.606	4.9	0.5	4.001	1.621	1750	171.8
Average	**2.459**		**5.6**	**0.6**	**4.002**	**1.577**	**1640**	**165.4**

Note: G_{mm} is based on one sample.

APPENDIX C –ONE-YEAR REVISIT TESTING DATA

Table C1 Volumetric Properties and Tensile Strength—HMA One-Year Cores

Sample	G_{mb}	G_{mm}	V_a, %	Water Absorption, %	Avg. Diameter, in.	Avg. Height, in.	Failure Load, lb.	Tensile Strength, psi
HCL-1	2.497	2.613	4.4	0.5	5.679	2.113	2100	111.4
HCL-2	2.488	2.613	4.8	0.6	5.681	1.788	1850	116.0
HCL-3	2.509	2.613	4.0	0.4	5.684	1.636	1700	116.3
HCL-4	2.507	2.613	4.0	0.4	5.669	1.644	--	--
HWP-1	2.514	2.613	3.8	0.4	5.678	1.662	1350	91.1
HWP-2	2.507	2.613	4.0	0.5	6.322	1.858	1700	92.1
HWP-3	2.519	2.613	3.6	0.5	5.633	1.761	1600	102.7
Average	**2.506**		**4.1**	**0.5**	**5.764**	**1.780**	**1717**	**104.9**

Note: G_{mm} is an average value, based on two samples (2.612 and 2.613).

Table C2 Volumetric Properties and Tensile Strength—WMA One-Year Cores

Sample	G_{mb}	G_{mm}	V_a, %	Water Absorption, %	Avg. Diameter, in.	Avg. Height, in.	Failure Load, lb.	Tensile Strength, psi
WCL-1	2.491	2.617	4.8	0.6	5.644	1.858	1800	109.3
WCL-2	2.486	2.617	5.0	0.6	5.653	1.864	1700	102.7
WCL-3	2.481	2.617	5.2	1.0	5.643	1.551	2300	167.3
WCL-4	2.482	2.617	5.2	0.9	5.660	1.406	--	
WWP-1	2.509	2.617	4.1	0.5	5.654	1.878	1900	114.0
WWP-2	2.492	2.617	4.8	0.7	5.650	2.056	2250	123.3
WWP-3	2.492	2.617	4.8	1.0	5.659	2.025	1900	105.5
Average	**2.490**		**4.8**	**0.7**	**5.652**	**1.805**	**1975**	**120.4**

Note: G_{mm} is an average value, based on two samples (2.616 and 2.617).

Table C3 Gradation and Asphalt Content—HMA One-Year Cores

	% Passing			
Sieve Size	**Sample 1**	**Sample 2**	**Average**	**Std. Deviation**
25.0 mm (1")	100.0	100.0	100.0	0.0
19.0 mm (3/4")	100.0	100.0	100.0	0.0
12.5 mm (1/2")	95.7	95.1	95.4	0.5
9.5 mm (3/8")	82.5	81.3	81.9	0.8
4.75 mm (#4)	52.5	51.3	51.9	0.8
2.36 mm (#8)	34.6	34.3	34.5	0.2
1.18 mm (#16)	24.9	25.4	25.2	0.3
0.6 mm (#30)	19.5	20.0	19.8	0.4
0.3 mm (#50)	16.2	16.7	16.5	0.4
0.15 mm (#100)	11.2	11.6	11.4	0.3
0.075 mm (#200)	7.5	7.9	7.7	0.3
	Sample 1	**Sample 2**	**Average**	**Std. Deviation**
Asphalt Content, %	5.79	5.97	5.88	0.13

Table C4 Gradation and Asphalt Content—WMA One-Year Cores

	% Passing			
Sieve Size	**Sample 1**	**Sample 2**	**Average**	**Std. Deviation**
25.0 mm (1")	100.0	100.0	100.0	0.0
19.0 mm (3/4")	100.0	100.0	100.0	0.0
12.5 mm (1/2")	94.4	93.7	94.1	0.5
9.5 mm (3/8")	80.7	80.5	80.6	0.2
4.75 mm (#4)	53.6	52.1	52.8	1.1
2.36 mm (#8)	37.0	36.1	36.5	0.7
1.18 mm (#16)	27.7	27.1	27.4	0.5
0.6 mm (#30)	22.2	21.6	21.9	0.4
0.3 mm (#50)	18.6	18.1	18.4	0.3
0.15 mm (#100)	12.7	12.3	12.5	0.3
0.075 mm (#200)	8.47	7.95	8.21	0.4
	Sample 1	**Sample 2**	**Average**	**Std. Deviation**
Asphalt Content, %	5.89	5.67	5.78	0.16

APPENDIX D – SUPPLEMENTAL PERFORMANCE TESTING DATA

Table D1 Master Curve Coefficients (AASHTO PP61-09)

Mix ID	Max E* (Ksi)	Delta	Beta	Gamma	E_A	R^2	S_e/S_y
Maxam Aquablack	3146.21	59.10	-0.415	-0.676	175368.9	0.996	0.046
HMA	3158.43	76.10	-0.046	-0.741	179585.8	0.976	0.110

Table D2 Raw Dynamic Modulus Data

Additive	Sample ID	Voids, %	Temp, C	Freq, Hz	Test Date	E*, ksi	δ, degrees
Maxam Aquablack	E506	7	4	10	8/5/2010	2021.8	11.11
Maxam Aquablack	E506	7	4	1	8/5/2010	1486.1	14.87
Maxam Aquablack	E506	7	4	0.1	8/5/2010	985.7	20.13
Maxam Aquablack	E506	7	20	10	8/6/2010	856.0	23.69
Maxam Aquablack	E506	7	20	1	8/6/2010	468.0	28.52
Maxam Aquablack	E506	7	20	0.1	8/6/2010	235.5	30.72
Maxam Aquablack	E506	7	40	10	8/6/2010	295.0	30.28
Maxam Aquablack	E506	7	40	1	8/6/2010	155.6	24.64
Maxam Aquablack	E506	7	40	0.1	8/6/2010	106.1	18.05
Maxam Aquablack	E506	7	40	0.01	8/6/2010	86.7	13.43
Maxam Aquablack	E508	7	4	10	8/5/2010	2154.0	10.89
Maxam Aquablack	E508	7	4	1	8/5/2010	1587.1	14.6
Maxam Aquablack	E508	7	4	0.1	8/5/2010	1053.4	19.98
Maxam Aquablack	E508	7	20	10	8/6/2010	870.7	24.86
Maxam Aquablack	E508	7	20	1	8/6/2010	466.0	29.6
Maxam Aquablack	E508	7	20	0.1	8/6/2010	235.5	30.88
Maxam Aquablack	E508	7	40	10	8/6/2010	303.9	31.83
Maxam Aquablack	E508	7	40	1	8/6/2010	160.0	26.78
Maxam Aquablack	E508	7	40	0.1	8/6/2010	110.6	20.57
Maxam Aquablack	E508	7	40	0.01	8/6/2010	93.5	14.91
Maxam Aquablack	E510	7.2	4	10	8/5/2010	2263.6	10.62
Maxam Aquablack	E510	7.2	4	1	8/5/2010	1672.9	14.43
Maxam Aquablack	E510	7.2	4	0.1	8/5/2010	1111.0	19.67
Maxam Aquablack	E510	7.2	20	10	8/6/2010	872.0	24.85
Maxam Aquablack	E510	7.2	20	1	8/6/2010	459.9	29.55
Maxam Aquablack	E510	7.2	20	0.1	8/6/2010	230.6	30.68
Maxam Aquablack	E510	7.2	40	10	8/6/2010	299.5	31.48

Maxam Aquablack	E510	7.2	40	1	8/6/2010	157.5	26.47
Maxam Aquablack	E510	7.2	40	0.1	8/6/2010	108.8	20.56
Maxam Aquablack	E510	7.2	40	0.01	8/6/2010	91.4	14.98
HMA	E555	7.2	4	10	8/5/2010	2082.0	10.86
HMA	E555	7.2	4	1	8/5/2010	1545.5	14.23
HMA	E555	7.2	4	0.1	8/5/2010	1051.2	18.94
HMA	E555	7.2	20	10	8/6/2010	1066.0	21.28
HMA	E555	7.2	20	1	8/6/2010	627.0	26.45
HMA	E555	7.2	20	0.1	8/6/2010	323.6	30.45
HMA	E555	7.2	40	10	8/13/2010	372.6	31.2
HMA	E555	7.2	40	1	8/13/2010	184.6	28.64
HMA	E555	7.2	40	0.1	8/13/2010	111.9	22.91
HMA	E555	7.2	40	0.01	8/13/2010	83.9	17.47
HMA	E556	7.1	4	10	8/5/2010	2248.8	10.74
HMA	E556	7.1	4	1	8/5/2010	1691.4	14.09
HMA	E556	7.1	4	0.1	8/5/2010	1153.9	18.82
HMA	E556	7.1	20	10	8/6/2010	1102.7	20.97
HMA	E556	7.1	20	1	8/6/2010	640.3	26.5
HMA	E556	7.1	20	0.1	8/6/2010	318.5	30.99
HMA	E556	7.1	40	10	8/13/2010	385.2	31.02
HMA	E556	7.1	40	1	8/13/2010	184.8	28.82
HMA	E556	7.1	40	0.1	8/13/2010	110.6	22.95
HMA	E556	7.1	40	0.01	8/13/2010	86.9	17.63
HMA	559	7.1	4	10	8/5/2010	2245.2	10.43
HMA	559	7.1	4	1	8/5/2010	1682.4	13.76
HMA	559	7.1	4	0.1	8/5/2010	1144.9	18.66
HMA	559	7.1	20	10	8/6/2010	1097.4	21.23
HMA	559	7.1	20	1	8/6/2010	637.6	26.59
HMA	559	7.1	20	0.1	8/6/2010	327.1	30.49
HMA	559	7.1	40	10	8/10/2010	318.5	31.63
HMA	559	7.1	40	1	8/10/2010	166.1	27.74
HMA	559	7.1	40	0.1	8/10/2010	111.2	22.49
HMA	559	7.1	40	0.01	8/10/2010	91.5	17.09

Table D3 Calculated Creep Compliance and Indirect Tensile Strength (IDT Test)

Test Temperature (deg C)	Loading Time (sec)	Creep Compliance (1/GPa)	
		WMA	HMA
-20	1	0.045	0.038
-20	2	0.046	0.04
-20	5	0.048	0.042
-20	10	0.051	0.045
-20	20	0.054	0.047
-20	50	0.059	0.051
-20	100	0.062	0.054
-10	1	0.065	0.054
-10	2	0.071	0.058
-10	5	0.079	0.065
-10	10	0.087	0.073
-10	20	0.095	0.081
-10	50	0.113	0.096
-10	100	0.129	0.11
0	1	0.121	0.084
0	2	0.137	0.094
0	5	0.167	0.12
0	10	0.194	0.142
0	20	0.237	0.172
0	50	0.312	0.234
0	100	0.4	0.302
Indirect Tensile Strength at -10C (MPa)		WMA	HMA
		3.77	4.03

Table D4 Maxwell Elements and Shift Factors for Critical Temperature Analysis

Maxwell Elements for Critical Temperature Analysis				
Index, i	WMA		HMA	
	λi (sec)	Ei (MPa)	λi (sec)	Ei (MPa)
1	12.775	4.433*10^3	10.107	5.243*10^3
2	185.627	4.745*10^3	128.938	3.941*10^3
3	2.73*10^3	4.259*10^3	1.487*10^3	4.537*10^3
4	3.35*10^4	4.25*10^3	1.281*10^4	6.195*10^3
5	9.974*10^5	4.699*10^3	3.075*10^5	6.2*10^3

Shift Factors for Creep Compliance Mastercurve (1/◦C)		
Temp (◦C)	WMA	HMA
-20	1	1
-10	141.254	125.893
0	10000	3162.278

Table D5 Individual Unconfined Flow Number Results

WMA Additive	Mix Heating	Sample ID	Sample Air Voids (%)	Francken Flow Number	Francken Microstrain
HMA	RH*	561	6.8	328	29893
HMA	RH	564	6.9	405	30437
HMA	RH	566	6.7	546	31198
HMA	Field**	81	6.8	254	32704
HMA	Field	82	6.5	436	32481
HMA	Field	84	6.9	305	34404
Maxam Aquablack	RH	512	7.2	221	32315
Maxam Aquablack	RH	513	7.4	241	30827
Maxam Aquablack	RH	514	7.3	218	31815
Maxam Aquablack	Field	6	7.4	180	31888
Maxam Aquablack	Field	23	6.9	185	31690
Maxam Aquablack	Field	29	6.7	234	29509

* RH denotes re-heated plant-produced mix compacted at the NCAT main laboratory
** Field denotes plant-produced mix that was compacted in the NCAT mobile laboratory

Table D6 Tukey-Kramer p-values ($\alpha = 0.05$) from Statistical Testing on Flow Number Data

Mix ID	**HMA - Field**	**HMA - RH**	**WMA - Field**	**WMA - RH**
HMA – Field	1.0	0.4494	0.2095	0.3693
HMA - RH		1.0	0.0238	0.0441
WMA – Field			1.0	0.9688
WMA – RH				1.0

Table D7 Individual Confined Flow Number Results

WMA Additive	**Sample ID**	**Sample Air Voids (%)**	**Test Temperature (^{o}C)**	**Microstrain at 20,000 cycles**	**Steady-State Rutting Slope**
Maxam Aquablack	E504	7.4	53	42965	0.6273
Maxam Aquablack	E507	7.5	53	51367	0.7666
Maxam Aquablack	E509	7.4	53	47324	0.6699
HMA (None)	E554	7.4	53	44503	0.6973
HMA (None)	E557	7.2	53	47456	0.7111
HMA (None)	E560	6.9	53	43102	0.6026